Romanian Reports in Physics, Vol. 67, No. 4, P. 1586–1596, 2015

Dedicated to
International Year of Light 2015

ANALYSIS OF OPTICAL MICROFIBER THERMAL PROCESSES

D. SAVASTRU[1], S. MICLOS[1], R. SAVASTRU[1], I. LANCRANJAN[1]

[1] National Institute of R&D for Optoelectronics INOE 2000, 409 Atomistilor Street, RO-077125, Magurele, Ilfov, Romania
E-mails: dsavas@inoe.ro, miclos@inoe.ro, rsavas@inoe.ro, j_j_f_l@yahoo.com

Received September 30, 2015

Abstract. Simulation results of thermal processes produced in bare SM optical fiber under longitudinal mechanical stress and heated with a source moving along it are presented. The purpose of this analysis was to study the thermal processes developed in the fiber during transforming into an optical microfiber-optic fiber nanowire.

Key words: optical microfiber, optical nanowire, adiabaticity criteria.

1. INTRODUCTION

Optical microfibers have attracted growing interest as components for photonic devices and integrated photonic systems dedicated to a vast domain of research, medical, industrial and security applications [1–4]. Optical microfibers are come under different names for instance tapered fibers (fiber tapers), subwavelength wires, micro-/nanowires, sub-micron diameter fibers, microfibers and nanofibers. They can be manufactured starting from single-mode fibers or bulk glass [5]. Optical microfibers have diameters are in the range of several tens of nanometers to several microns. Optical microfibers have many unique characteristics such as strong evanescent field, flexible, high nonlinearity, high configurability, and controllable dispersion. Low-loss microfibers has opened up new opportunities for various micro-photonic devices including micro-resonators, fiber couplers [2], and industrial sensors [3, 4] using microfibers. Bi-conical tapered fibers (Fig. 1) that preserve their low loss connection with the original single mode fibers (SMF) provide the greatest advantage of achieving low-loss micro-photonic devices. In the category micro/nano photonic devices are included also the single conical tapered fibers. Optical microfibers have performance comparable with the ones of optical planar waveguides [5]. As a functional photonic component, microfiber structures can be operated in the form of loop, knot and coil, with unique optical quality. A microfiber loop resonator (MLR) can reach a Q-factor of 120,000 [6]. Optical microfibers have applications including optical communications, laser systems [7], optical signal processing [8, 9], spectroscopy, industrial sensors for temperature, refractive index, chemistry,

biomedical and pressure. An application which has been commercially available for decades based on the use of optical microfiber consists in optical fiber couplers. When two microfibers are put in close contact, the strong evanescent fields of these two microfibers allow exchange of energy between them. Splitting or combining of light power can be realized in fibers using fiber couplers. The same mechanism is involved in many other optical microfiber devices such as microfiber loop resonator (MLR) [10, 11], microfiber coil resonator (MCR) [5, 12–14], microfiber knot resonator (MKR) [1, 3, 15], reef knot microfiber resonator as an add/drop filter [16], microfiber Mach-Zehnder interferometer (MMZI) [17, 18], microfiber loop mirror [19], miniature lasers [6, 20], optical filters [16, 21] and dispersion compensating [22, 23]. The most useful characteristic of optical microfibers that makes them ultra-sensitive to ambient media is their strong evanescent field. However, it is difficult to exploit this property without integrating them with external interferometry or making optical microfibers as parts of interferometer or resonator configurations.

A schematic representation of a bi-conical optical microfiber (OMF) is presented in Fig. 1. As it is represented, an optical microfiber consists into a modified segment of a single mode (SM) fiber. It has a Down-taper, a Waist and an Up-taper. Along the Down-taper, the initial cladding diameter of usually/standard 125 μm is lowered 10–50 times down to the Waist diameter of 0.5–1.0 μm. The Waist has a constant diameter. After that, along the Up-taper, the OMF diameter increase up to the SM initial 125 μm diameter. Along the Down-taper and Up-taper, the OMF diameter varies with displacement along the fiber approximately as a slow exponential law. Usually, because of ease of fabrication and exploitation reasons the Down-taper and Up-taper are symmetric, with the same length which can be several tenths up to 1000 time longer than the Waist length. The Waist length is usually not longer than 5–7 mm.

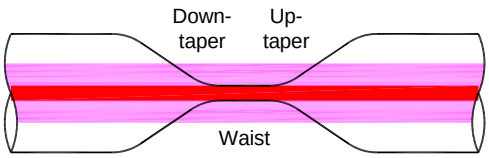

Fig. 1 – Schematic representation of OMF shape. The initial fiber diameter is connected to the waist section via two symmetric tapers.

Since their first experimental application, OMF have been manufactured using various techniques: laser ablation [24], sapphire tube micro furnace with the SM fiber introduced in it and heated with CO_2 laser [25], electron beam lithography [26], vapor–liquid–solid techniques [27], and fiber pulling [28, 29] or direct draw from bulk glasses [30]. Among those methods, the flame heating technique has proven to be the best method as it can produce microfiber with the best physical properties [28, 31]. In this paper, simulation results obtained

considering the most used microfiber fabrication techniques, namely flame brushing technique [31] are presented. However, flame brushing technique appears to be the major technique used in the fabrication of tapered fiber.

The simulation results presented in this paper were obtained with the purpose of improving the designs of OMF fabrication installation and of sensing devices based on optical microfibers use. The simulation procedure is aiming to regular SM optic fibers which can be thermally processed into OMF/OFN by applying in a PC controlled procedure a necessary amount of energy obtained from a heat brush. The main purpose of the accomplished preliminary analysis of thermal processes produced into a SM optic fiber when transforming it into an optic fiber nanowire. The analysis consists in generating two types of output files: one formed by coordinate pairs, referring to the hot zone (the future Waist, the position on the optic fiber axes and the optic fiber diameter and the other (which are not presented) formed by numerical, binary instruction codes to be inscribed into the memory of a microcontroller which, has the role to coordinate the relative positions of the processed optic fiber and the thermal energy source.

2. OPTICAL MICROFIBER CHARACTERISTICS

The increasing number of OMF's various applications results from their optical properties, which are due to an important feature of their geometric structure, which consists in keeping constant the ratio of cladding and core diameters along the input and output initial SM fibers, the Down-taper, the Up-taper and the Waist. Due to the small cross section of the OMF Waist (Fig. 1) about 50 % or more of power guided through it propagates outside the physical boundary of the OMF as an evanescent field. This evanescent field can be accessed rather easily for experiments and offers high light sensitivity because of the strong spatial confinement. Regular optical fiber main characteristic – weakly guiding caused by the low differences between the values of core and clad refractive index losses its significance in the Waist and tapers segments of an OMF. The field energy of the fundamental transverse fiber mode (HE_{11}) propagates in the core of the fiber and only hardly extends into the cladding. In the Waist and tapers of an OMF the field energy can be confined into the core because of its diameter smaller than the propagating light wavelength and, as a consequence is guided by the boundary of fiber cladding and surrounding medium, usually air. As a consequence, the weak guidance changes to strong guidance because of the orders of magnitude larger relative refractive indexes difference between cladding and surrounding medium.

Coming to this point it is important to mention the most important OMF theoretical clue, due to which its increasing number of application is possible. This theoretical clue is the adiabaticity criteria [32] according to which the power of fundamental mode in the SMF is conserved as much as possible during propagation through OMF tapers of varying radius by preventing the mode-interaction between

it with the higher order modes. Adiabatic tapered fibers can be fabricated by ensuring the shape of tapered fiber fulfills the adiabaticity criteria. For short, higher order modes will be suppressed when entering taper waists of small radii and they lose power. Therefore, adiabaticity is crucially important when it comes to fabrication of single-mode OMF and will be the subject of a future paper.

OMF offers another important property which is the large evanescent field. The variation of mode field diameter (MFD) in the varying tapered fiber diameter was discussed by Love [33]. In a conventional SMF, the fundamental mode field can be described with a fair approximation by Gaussian distribution where a significant large fraction of field power is confined within the core of fiber and a small fraction of modal power is in the cladding near to the core-cladding boundary. The MFD is that at which the power of the field $1/e^2$ of maximum intensity of the mode. MFD has a strong dependency on the diameter and numerical aperture (NA) of the tapered fiber. Their relationship can be well-related through V number as given by

$$V = \frac{2\pi\rho \mathrm{NA}}{\lambda}, \tag{1}$$

where ρ is the core/cladding radius of the tapered fiber. In Chapter 4, the results obtained regarding the MFD variation will be presented.

3. OPTIC FIBER TAPERING MODEL

For further investigation the fiber is assumed to have a hot zone of constant length L. In this zone the viscosity of the fiber is assumed to be uniform and significantly lower than in the rest of the considered fiber. This reflects the strong temperature dependence of fused silica viscosity. Let the initial fiber diameter along the hot zone be D_0. For the infinitesimal elongation δx and the resulting negative change in fiber diameter δD, the conservation of mass can be expressed as

$$\frac{\pi}{4} D_0^2 L = \frac{\pi}{4} \left(D_0 + \delta D \right)^2 \left(L + \delta x \right). \tag{2}$$

It comes to application when the bare fiber material is locally heated and the viscosity lowers so that it allows deformation. The latter is introduced by a symmetric pulling force. It acts on the fiber ends along their axis and thus causes the fiber diameter to shrink in the hot section. Effects of thermal expansion or evaporation of the optic fiber constituent material, fused silica, can be neglected.

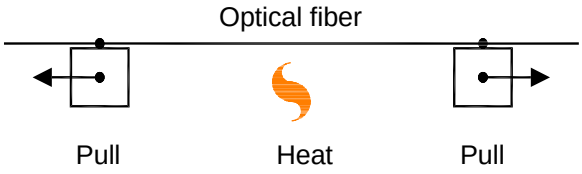

Fig. 2 – Schematic representation of the analyzed process. Tapering of the optical fiber by pulling the ends apart while the fiber material is locally heated by a thermal energy source.

The optic fiber elongations, δx, and the resulting negative change in fiber diameter, δD, are considered as infinitesimal. As a consequence, only linear terms are considered after expanding the previous equation. The resulting differential equation is

$$\frac{\mathrm{d}D}{\mathrm{d}x} = -\frac{D}{2L}. \tag{3}$$

For this simple differential equation, the initial fiber diameter is defined as the initial condition:

$$D_0 = D\left(x = 0\right). \tag{4}$$

The integration of the above differential equations yields:

$$D\left(x\right) = D_0 \exp\left(-\frac{x}{2L}\right). \tag{5}$$

The optic fiber elongation, δx, and the resulting negative change in fiber diameter, δD, are considered as infinitesimal. As a consequence, only linear terms are considered after expanding the previous equation. The resulting differential equation is.

So, the idea of simple fiber pulling leads to a very limited variety of possible shapes of OMFs. Any waist diameter can be reached by selecting the fiber elongation x accordingly. But the resulting taper shape is always exponential for a constant hot fiber zone L. This is because with every elementary elongation step the current fiber diameter is pulled out of the hot zone. An exponential taper is obtained. Consequently, in the approach of simple fiber pulling either the length of the waist or that of the taper can be considered as a degree of freedom. The length of the OMF waist equals the length of the hot fiber zone. Once the final elongation is reached, the hot zone is the only section of constant diameter. The developed model allows the use a previous experience in simulation of laser material micro-processing [34, 35] and design of fiber optic sensors dedicated to specified applications [36–41] for improved design of OMF sensors.

4. SIMULATION RESULTS

The simulation process was performed into two stages. The presented results were obtained considering the heat brush as the OMF manufacturing technique. The first one consists in evaluation of light propagation through OMF parameters. The results obtained in the first stage allow the definition of OMF shape specification (mainly the Waist and tapers lengths) which is imposed by a previously designated application. The second stage consists in an evaluation of OMF shape and other parameters of interest and of heat brush passes over the Waist segment.

Figures 3–5 show the variation plot of absolute fiber mode spot size *vs.* the *V* number of a tapered fiber for light propagation at wavelengths 633 nm, 1064 nm and 1550 nm and considering an initial SMF diameter of 8.4 μm. For all three wavelengths, the absolute fiber mode spot variations versus *V* number have the same characteristics. As seen in Figs. 3–5, the MFD is decreasing with the decreasing core diameter and it reaches its minimum at $V_{\text{core}} \approx 2$. As the radius of the fiber continues to decrease, the diffraction effect begins to dominate and the MFD begins to increase. Until certain point where the effective index of the fundamental mode in the fiber core is equivalent to that of cladding, the confining effect has countered the effect of diffraction and the MFD is decreasing again. Starting from this point, the light in the fiber is guided by air-cladding interface and the effect of the core can be neglected. The MFD reaches the minimum again when $V_{\text{cladding}} \approx 2$. The nonlinear effect is optimum at this point because of the strong confinement of light intensity within this tapered fiber. The MFD is increasing monotonically with decreasing cladding diameter. The mode field spreads out of the cladding of the fiber forming the fiber evanescent field. Typically, stronger evanescent field can be achieved with a tapered fiber of smaller radius and the power in the evanescent field can reach as much as 90% of the total power.

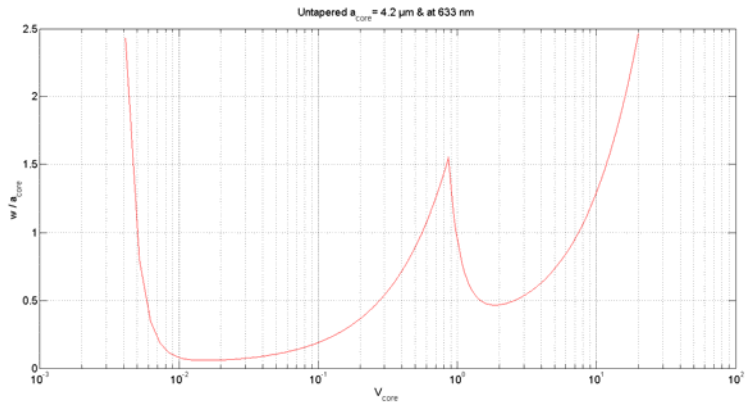

Fig. 3 – Variation of absolute fiber mode spot size *vs.* the *V* number of a tapered fiber at 633 nm.

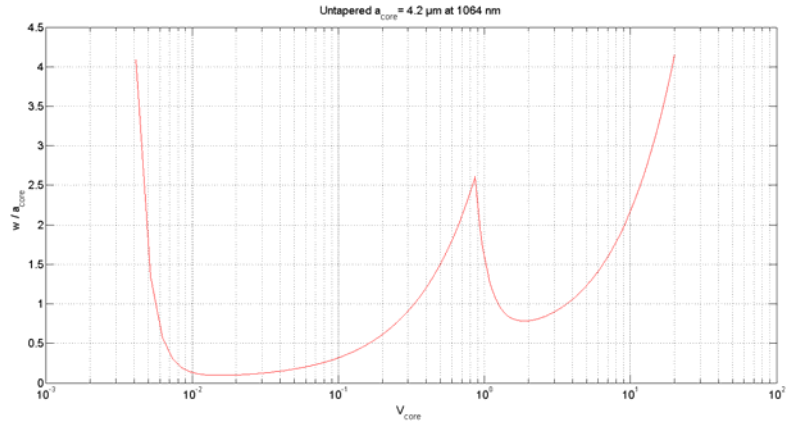

Fig. 4 – Variation of absolute fiber mode spot size *vs.* the *V* number of a tapered fiber at 1064 nm.

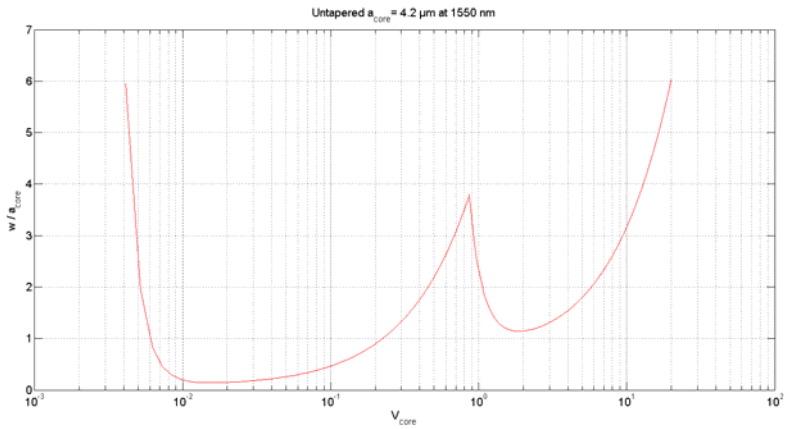

Fig. 5 – Variation of absolute fiber mode spot size *vs.* the *V* number of a tapered fiber at 1550 nm.

It is worth to be noticed that the confinement of light power within micro-/ nanofiber decreases with decreasing diameter which results to strong evanescent field. This effect is wavelength dependent and the longer wavelength has stronger evanescent field.

Figures 6–10 present the simulation results obtained using the optic fiber tapering model, more precisely the equations (2–5) which define the developed simulation model. The simulations were obtained in the case of a silica glass SM fiber having a core diameter of 11.2 μm and an initial cladding fiber diameter of 125 μm. The final parameters were: 0.35 μm waist diameter and 7500 μm waist length. The typical fiber elongation rate is considered to be about 100 μm/s. The

averaged over an entire trip (including acceleration and deceleration) flame move velocity is approximately 2.5 mm/s. The flame peak velocity is considered to be less than 4 mm/s because of the heating time constant of the optical fiber. In Figs. 6–10 the main parameters of interest for OMF fabrication process are presented: correspondingly the fiber diameter versus OMF coordinate; hot zone size versus taper coordinate; fiber elongation versus taper coordinate; hot zone size (pulling process) versus taper coordinate; flame oscillations (pulling process) versus fiber elongation.

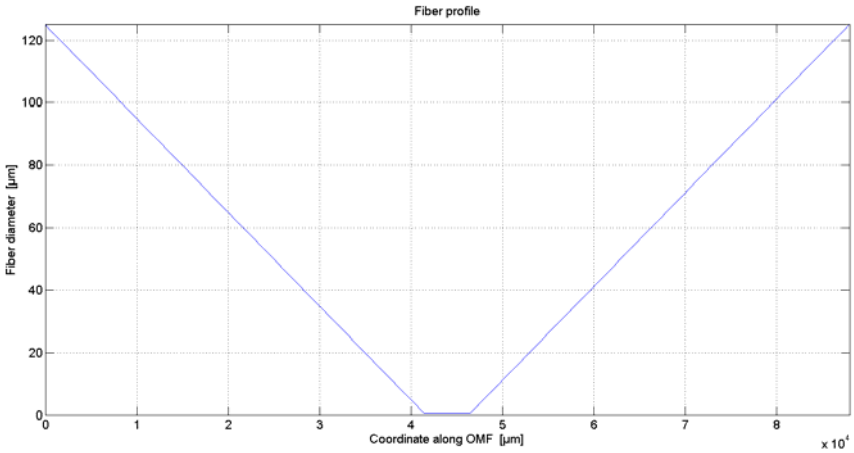

Fig. 6 – Fiber profile. Variation of fiber diameter *vs.* coordinate along OMF.

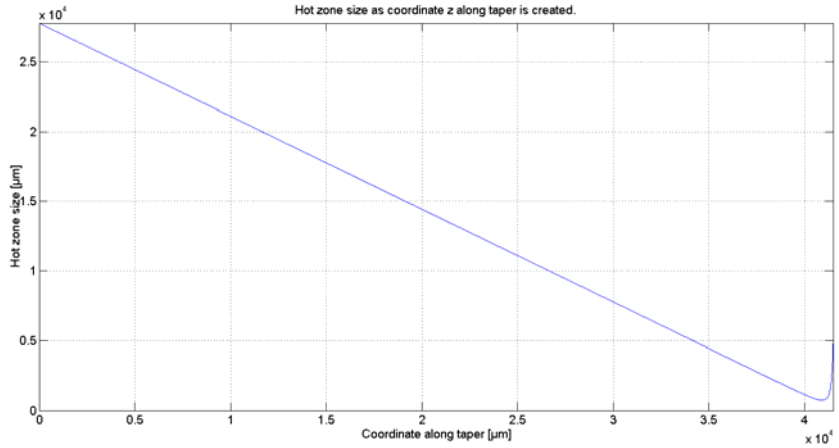

Fig. 7 – Hot zone size as coordinate along taper is created. Variation of hot zone size *vs.* coordinate along taper.

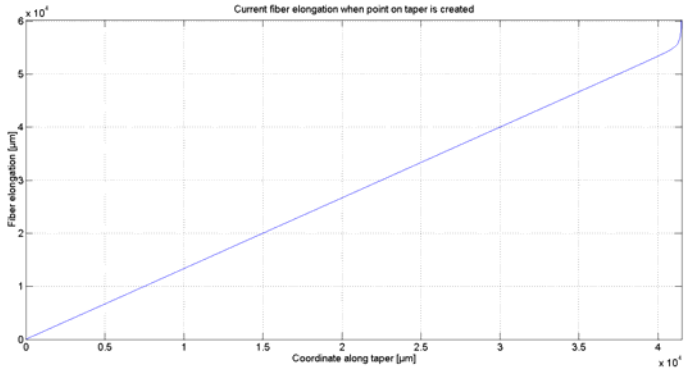

Fig. 8 – Current fiber elongation when point on taper is created.
Variation of fiber elongation *vs.* coordinate along taper.

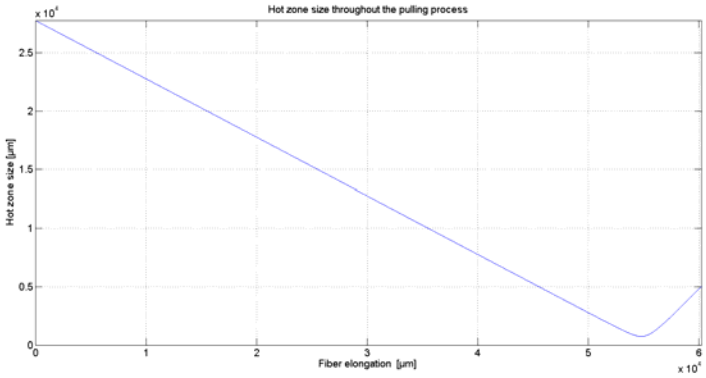

Fig. 9 – Hot zone size through pulling process. Variation of hot zone size *vs.* fiber elongation.

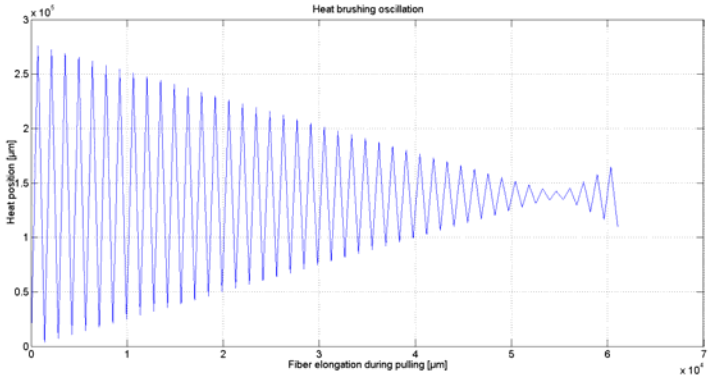

Fig. 10 – Heat Brush Oscillations – variation of heat position (flame position)
vs. fiber elongation during pulling.

5. CONCLUSIONS

The main purpose of the performed analysis consists in investigation of thermal processes developed in the optic fiber during transforming into an optical microfiber-optic fiber nanowire (OMF/OFN) and its optic parameters.

The results obtained in the first stage of the simulation (evaluation of light propagation through OMF parameters allow the definition of OMF shape specification (mainly the Waist and tapers lengths) which is imposed by a previously designated application.

In the second stage (evaluation of OMF shape and other parameters of interest and of heat brush passes over the Waist segment) the main parameters of interest for OMF fabrication process are obtained: correspondingly the fiber diameter versus OMF coordinate, hot zone size versus taper coordinate, fiber elongation versus taper coordinate, hot zone size (pulling process) versus taper coordinate, flame oscillations (pulling process) versus fiber elongation.

It was demonstrated the correlation between OMF/OFN heat source necessary parameter specification and the optic fiber parameters to be obtained.

Acknowledgments. This work was financed by the Romanian Ministry of Education and Scientific Research by means of the Research Program No. PN 09-27.02.03.

REFERENCES

1. X. Jiang, L. Tong, G. Vienne, X. Guo, A. Tsao, Q. Yang, D. Yang, App. Phys. Lett. **88**, 223501 (2006).
2. Y. Jung, G. Brambilla, D. J. Richardson, Opt. Express **17**, 5273 (2009).
3. K. S. Lim, S. W. Harun, S. S. A. Damanhuri, A. A. Jasim, C. K. Tio, H. Ahmad, Sensors and Actuators A: Phys. **167**, 377 (2011).
4. X. Zeng, Y. Wu, C. Hou, J. Bai, and G. Yang, Opt. Comm. **282**, 3817 (2009).
5. L. Tong, L. Hu, J. Zhang, J. Qiu, Q. Yang, J. Lou, Y. Shen, J. He, Z. Ye, Opt. Express **14**, 82 (2006).
6. M. Sumetsky, J. Lightwave Technol. **26**, 21 (2008).
7. M. Sumetsky, Y. Dulashko, J. M. Fini, A. Hale, D. J. DiGiovanni, J. Lightwave Technol. **24**, 242 (2006).
8. X. Jiang, Q. Song, L. Xu, J. Fu, L. Tong, App. Phys. Lett. **90**, 233501 (2007).
9. K. Amarnath, R. Grover, S. Kanakaraju, H. Ping-Tong, Phot. Technol. Lett. **17**, 2280 (2005).
10. S. W. Harun, K. S. Lim, A. A. Jasim, H. Ahmad, J. Mod. Opt., **57**, 2111 (2010).
11. S. Harun, K. Lim, A. Jasim, and H. Ahmad, Las. Phys. **20**, 1629 (2010).
12. M. Sumetsky, Y. Dulashko, J. M. Fini, A. Hale, Appl. Phys. Lett. **86**, 161108 (2005).
13. M. Sumetsky, Y. Dulashko, S. Ghalmi, Opt. and Las. in Eng. **48**, 272 (2010).
14. F. Xu and G. Brambilla, Opt. Lett. **32**, 2164 (2007).
15. F. Xu, P. Horak, G. Brambilla, Opt. Express **15**, 7888 (2007).
16. Y. Wu, Y.-J. Rao, Y.-h. Chen, and Y. Gong, Opt. Express **17**, 18142 (2009).
17. G. Vienne, A. Coillet, P. Grelu, M. El Amraoui, J.-C. Jules, F. Smektala, L. Tong, Opt. Express **17**, 6224 (2009).
18. Y.-H. Chen, Yu Wu, Y.-J. Rao, Q Deng, Y Gong, Opt. Comm. **283**, 4 (2010).

19. Y. Li and L. Tong, Opt. Lett. **33**, 303 (2008).
20. J. Xiaoshun, T. Limin, S. Qinghai, X. Lei, in *Conference on Lasers and Electro-Optics* (CLEO 2007), 1 (2007).
21. X. Jiang, Y. Chen, G. Vienne, and L. Tong, Opt. Lett. **32**, 1710 (2007).
22. C. K. Madsen and G. Lenz, Phot. Technol. Lett. **10**, 994 (1998).
23. O. Schwelb, J. Lightwave Technol. **22**, 1380 (2004).
24. A. M. Morales and C. M. Lieber, Science **279**, 208 (1998).
25. M. Sumetsky, Y. Dulashko, and A. Hale, Opt. Express **12**, 3521 (2004).
26. J. Chen, M. A. Reed, A. M. Rawlett, and J. M. Tour, Science **286**, 1550 (1999).
27. J. Westwater, D. P. Gosain, S. Tomiya, S. Usui, H. Ruda, J. Vac. Sci. and Technol. B: Microel. and Nanometer Struct. **15**, 554 (1997).
28. G. Brambilla, V. Finazzi, D. Richardson, Opt. Express **12**, 2258-2263 (2004).
29. A. M. Clohessy, N. Healy, D. F. Murphy, C. D. Hussey, Electr. Lett. **41**, 954 (2005).
30. X. Xing, Y. Wang, B. Li, Opt. Express **16**, 10815 (2008).
31. S. Harun, K. Lim, A. Jasim, H. Ahmad, Laser Physics **20**, 1629 (2010).
32. T. A. Birks and Y. W. Li, J. Lightwave Technol. **10**, 432 (1992).
33. J. D. Love, Electr. Lett. **23**, 993 (1987).
34. D. Savastru, A. Vlase, I. Lancranjan, R. Savastru, S. Miclos, U. P. B. Sci. Bull.-Ser. A **73**, 167 (2011).
35. D. Savastru, R. Savastru, I. Lancranjan, S. Miclos, C. Opran, Proceedings of SPIE **8882**, 88820S (2013).
36. R. Savastru, I. I. Lancranjan, D. Savastru, S. Miclos, Proceedings of SPIE **8882**, 88820Y (2013).
37. I. Lancranjan, S. Miclos, D. Savastru, R. Savastru, C. Opran, Proceedings of SPIE **8433**, 843315 (2012).
38. I. Lancranjan, S. Miclos, D. Savastru, J. Opt. Adv. Mat. **12**, 1636 (2010).
39. I. Lancranjan, S. Miclos, D. Savastru, A. Popescu, J. Opt. Adv. Mat. **12**, 2456 (2010).
40. S. Miclos, D. Savastru, R. Savastru, I. I. Lancranjan, Proceedings of SPIE **9517**, 95172B (2015).
41. D. Savastru, S. Miclos, R. Savastru, I. I. Lancranjan, Proceedings of SPIE **9517**, 95172A (2015).